Deep inelastic separated response functions from ^{40}Ca and ^{48}Ca

M. Deady* and C. F. Williamson
Department of Physics and Bates Linear Accelerator Center, Massachusetts Institute of Technology, Cambridge, Massachusetts 02139

P. D. Zimmerman
Department of Physics and Astronomy, Louisiana State University, Baton Rouge, Louisiana 70803

R. Altemus and R. R. Whitney
Department of Physics, University of Virginia, Charlottesville, Virginia 22901
(Received 29 January 1986)

Deep inelastic scattering cross sections have been measured for ^{40}Ca and ^{48}Ca at electron energies between 100 and 375 MeV at scattering angles of 90° and 140°. Longitudinal and transverse response functions at three-momentum transfers between 250 and 410 MeV/c have been extracted using a Rosenbluth separation. The response functions are compared to calculations modeling the nucleus as a noninteracting relativistic Fermi gas. The model is found to agree with the observed transverse response function in the region of expected quasi-free nucleon knockout, but the model overestimates the observed longitudinal response. Comparisons of the response functions of the two isotopes are made, and differences between ^{40}Ca and ^{48}Ca are seen.

INTRODUCTION

Inclusive electron scattering experiments that cover a large range of energy loss, ω, make possible the investigation of many modes of excitation of the nucleus. As ω increases, the nucleus is observed to have bound states, collective resonance structures, and nucleon knockout. Once the Δ-production threshold has been passed, both mesonic and nucleonic degrees of freedom become important. The deep inelastic region provides an opportunity to observe the response function of the nucleon in the mean field produced by the other nucleons in the nucleus. Comparisons with the response function of a free nucleon could give insights into nucleon-nucleon interactions as well as any modifications of the properties of the nucleon itself in this environment.

By performing scattering experiments at different laboratory angles, components of the excitation which result from the electron's interactions with the charge and with the current and/or spin of the nucleus can be distinguished. These Rosenbluth type of separations into longitudinal and transverse response functions should make it easier to identify the character of the excitations, since certain effects should exhibit a particular signature. Mesonic effects, for instance, would presumably be important only in the transverse response function.

The predominant effect in the kinematic region covered by this experiment is expected to be the scattering of the electron from a single nucleon, resulting in the knockout of the nucleon from the nucleus. In earlier experiments[1,2] the general characteristics of the cross section in this region were well explained by models assuming the nucleon was in a quasi-free initial state. The primary interaction between nucleons in these models is the Pauli exclusion principle, which determines the possible final states of the struck nucleon. The effect of the other nucleons was taken into account by the use of an average binding energy or an effective mass for the struck nucleon.[3] Further refinements, such as describing the initial nucleon by a more realistic shell model wave function, result in minor modifications to the predicted response.[4,5]

Recent experiments have yielded separated response functions for a few target nuclei, such as ^{12}C (Ref. 6), ^{40}Ca and ^{48}Ca (Refs. 7–9), and ^{56}Fe (Refs. 8 and 9). New experiments in larger kinematic regions on these nuclei and ^{238}U (Ref. 10) are underway. The completed experiments show a distinct difference in the separated response functions from the relatively simple behavior observed in the total cross sections.

In this paper, we present the results of our studies on ^{40}Ca and ^{48}Ca. The separated response functions are compared with the predictions of a simple model of the nucleon knockout process as a useful benchmark. Some comparison of the response of the two isotopes is performed, in an attempt to detect any effects in the response functions due to the large neutron number difference.

EXPERIMENTAL PROCEDURE

The experiment was performed at the Bates Linear Accelerator Center. Electrons ranging in initial energy from 100 to 375 MeV were scattered from a target of natural calcium and a target that had been enriched to the level of 98% in ^{48}Ca. The scattered electrons were momentum analyzed by the 900 MeV/c energy loss spectrometer system (ELSSY), using the standard Bates system of multiwire proportional chambers and Lucite Čerenkov detectors.[11] The largest uncertainty in these measurements is that resulting from a lack of knowledge of the precise effective target thickness. This, and other uncertainties due

to the experimental setup are accounted for in the assignment of a 4% systematic uncertainty to the measured cross sections.

The overall efficiency of the system was determined by comparison of scattering from hydrogen in a polyethylene target with the calculated electron-proton cross section. These comparisons indicated that no renormalization of the data was needed. In a few cases, data were taken under the same kinematic conditions at different times. These data agreed in absolute magnitude to within 2% for spectra taken as much as three years apart.

At incident energies greater than 250 MeV, a significant background of pions that were energetic enough to trigger the Lucite Čerenkov counters was observed. Some of the data obtained later were taken with a silica aerogel Čerenkov detector substituted for one of the Lucite detectors. The substitution of aerogel ($n=1.05$) for Lucite ($n=1.49$) prevented pions bent into the detector system by the spectrometer magnet from triggering the detectors. For those energies at which no data with the aerogel detector were taken, a determination of the pion component was made from a measurement of the positive pion cross section when the magnet polarity was reversed.

Data were taken for a total of seven incident energies at a scattering angle of 90° and for nine energies at 140°. There were also runs at 160° where the cross section would be almost entirely transverse. In a few cases, these data were used as a consistency check on the Rosenbluth separations, and the linearity confirmed that the effects of Coulomb distortions are small for low-Z nuclei. The separations were performed entirely from the 90° and 140° data sets.

ANALYSIS

The extraction of cross sections to be used for a Rosenbluth separation involved many steps of analysis. Some of these corrections were determined experimentally, some theoretically. Each contributed to the assignment of an overall systematic error based on the confidence of the experimenters in the correction. Figure 1(a) shows a typical spectrum and some of the more important corrections. Figure 1(b) compares an uncorrected spectrum with a completely corrected spectrum.

Some data had been taken with the polarity of the spectrometer magnet reversed. These spectra, showing both positive pions and positrons pair-produced in the target, were used to determine subtractive corrections to the data for the presence of negative pions and pair-produced electrons in the normal polarity spectra. The pair-produced electron cross section was assumed to be identical to the observed positron contribution to the reversed polarity runs, and a direct subtraction of a fit to the positron cross section was performed. This correction was only important at final electron energies less than 100 MeV, and never amounted to more than 10% of the measured cross section.

The pion contribution was important at incident energies greater than 250 MeV and energy losses greater than 150 MeV. For those spectra that were taken with the aerogel counter, no correction for pions was necessary. A comparison of these pion-free spectra with spectra taken under the same conditions with the Lucite counters allowed a determination of the best way to correct for the pion contribution in the spectra. The observed positive

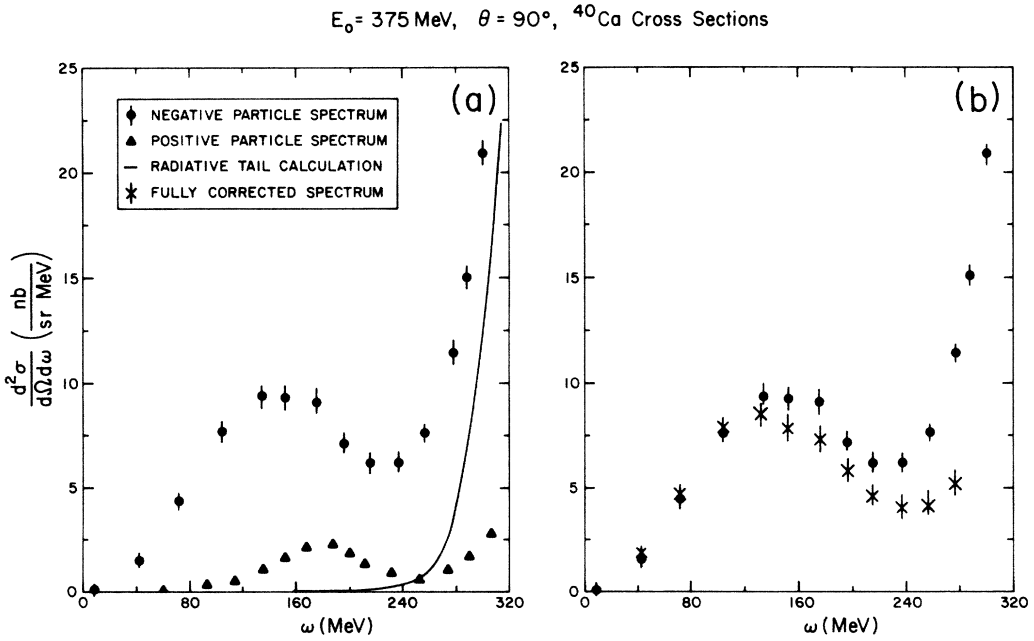

FIG. 1. Experimental cross sections for ^{40}Ca with $E_0=375$ MeV and $\theta=90°$. (a) Cross sections for negative particles are given by circles, those for positive particles are given by triangles, and the solid curve indicates the calculation of the radiative tail of the elastic peak. (b) The negative particle spectrum is again given by circles, the fully corrected spectrum is given by asterisks. Systematic errors are shown throughout.

pion component of the reversed polarity spectra took the form of a peak that amounted to 25% of the normal polarity cross section in the worst cases, and considerably less than that in most cases. A fit to this peak, multiplied by various scale factors, was subtracted from the negative particle spectrum. A scale factor of 1.0 yielded the best agreement with the aerogel spectra, indicating that the negative pion contribution was essentially equal to the positive pion contribution. Spectra for which no aerogel data existed were then corrected by subtracting a fit to the positive pion component of the reversed polarity spectrum at the same energy and angle, with a scale factor of unity for the pion peak.

Low energy electrons were found to have a lower detection efficiency in the Lucite detectors due to energy losses in passing through the detectors. This necessitated a correction to the overall efficiency of the detector system for final electron energies less than 110 MeV. The correction amounted to roughly 2% at 110 MeV final electron energy and 6% at 80 MeV. The correction was determined by a comparison of the relative efficiency of the detection system with various combinations of the Lucite and aerogel Čerenkov counters.

A persistent background effect was found to have been caused by electrons scattered into the spectrometer from the target chamber aperture.[12] Measurements were performed with a new chamber, whose aperture was sufficiently wide that such scattering could not produce an event at the focal plane. The differences between the spectra taken with the old and new chambers could be described quite adequately by a theoretical correction based on a calculation of multiple scattering and thick-target bremsstrahlung in the chamber walls. This correction was as large as 18% in the region of 50—100 MeV of energy loss. Detailed accounts of the origin of this background and the correction calculation are found in Ref. 12.

Radiative effects which distort the electron spectrum must be calculated. The radiative tail due to elastic scattering, a significant contribution at the lowest final electron energies, was calculated using the "exact" first Born formalism of Mo and Tsai,[13] which includes both internal and external bremsstrahlung. A recent direct measurement of the radiation tail[14] from tungsten demonstrated that even for heavy nuclei, this procedure is accurate to within a few percent of the calculated radiative tail down to quite low final electron energies.

Primarily because of uncertainties with corrections at low final electron energies, no data with final electron energies less than 80 MeV were kept in the final corrected cross sections. This limited the dependence of the final results on many of the corrections. For instance, for no data points included in the final separations were the radiative tail subtractions more than 20% of the measured cross sections.

Once the radiative effects due to elastic scattering were eliminated, those due to inelastic scattering had to be dealt with. The inelastic cross sections at each energy and angle were radiatively unfolded according to the method detailed by Miller,[15] based upon the continuum correction technique developed by Mo and Tsai.[13] The change in the cross section due to this correction was always less than 5% in the deep inelastic region.

At this point in the analysis, there were, in hand, double differential cross sections over a wide range of momentum transfer, q, and energy loss, ω, at scattering angles of 90° and 140° with all corrections performed. Response functions for each angle at constant q were extracted by linear interpolation between the data points, with no extrapolations being performed. The interpolation was done in two steps. First, response functions were found at evenly spaced values of ω for each constant energy spectrum. Next, for each value of ω, response functions were found at the desired values of q by using the data from the two nearest spectra. The Kawazoe scaling variable y (Ref. 16) was used as an interpolation variable in this second step, since it lined up the centers of the quasi-elastic peaks of different spectra, increasing the smoothness of the variations. The reliability of the interpolation was checked by trying different interpolation variables, by cubic interpolation, and by analyzing pseudodata generated from Fermi gas calculations. All tests yielded consistent and stable results, and it was concluded that no spurious effects arose from the data analysis.

These response functions were then used to determine the longitudinal (charge) and transverse (spin and current) response functions according to the formula,

$$\frac{d^2\sigma}{d\Omega\, d\omega} = \frac{4\pi}{M_T}\sigma_{\text{Mott}}\left\{\left[\frac{q_\mu^2}{q^2}\right]^2 S_L(q,\omega) + \left[\frac{1}{2}\left[\frac{q_\mu^2}{q^2}\right] + \tan^2\left[\frac{\theta}{2}\right]\right] S_T(q,\omega)\right\},$$

where σ_{Mott} is the Mott cross section, M_T is the target mass, q_μ is the four-momentum transfer, q is the three-momentum transfer, ω is the energy transfer, θ is the laboratory scattering angle, S_L and S_T are, respectively, the longitudinal and transverse response functions, and $d^2\sigma/d\Omega\, d\omega$ is the double differential cross section. Throughout the analysis, systematic and statistical errors were treated and are reported separately.

SEPARATED RESPONSE FUNCTIONS

The longitudinal and transverse response functions for both ^{40}Ca and ^{48}Ca, as determined by the Rosenbluth separation, are presented in Fig. 2. While this is the first presentation of deep inelastic scattering results for ^{48}Ca from data taken at Bates, separations for ^{40}Ca have been presented for some of these values of momentum transfer in a previous publication.[7] The present results differ from those in only one significant respect. These results include an improved determination of the cross sections at 350 MeV initial electron energy and 90° based on a reanalysis of all of the data taken with the aerogel detector. The main result of that reanalysis is a reduction of the longitudinal response functions at the highest momentum transfers.

The results of calculations of the Fermi gas model of the nucleus, according to the method of Van Orden and

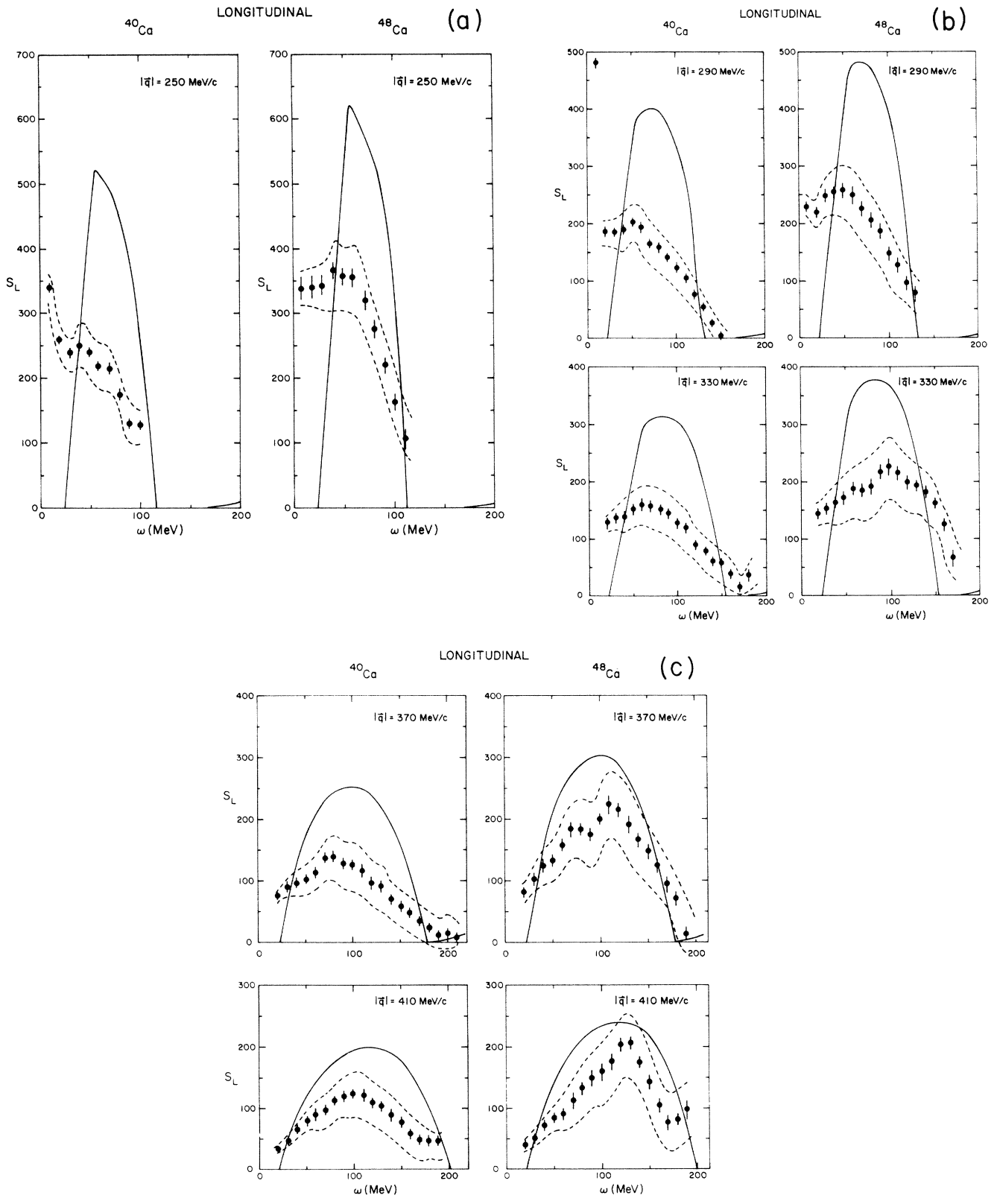

FIG. 2. Separated response functions compared to Fermi gas calculations of Van Orden, including mesonic effects. Standard deviations due to statistical errors are indicated by error bars, the dotted lines indicate a systematic error band, and the solid line is the calculation of Van Orden. (a) Longitudinal response functions for $|\mathbf{q}| = 250$ MeV/c. (b) Longitudinal response functions for $|\mathbf{q}| = 290$ and 330 MeV/c. (c) Longitudinal response functions for $|\mathbf{q}| = 370$ and 410 MeV/c. (d) Transverse response functions for $|\mathbf{q}| = 250$ and 290 MeV/c. (e) Transverse response functions for $|\mathbf{q}| = 330$, 370, and 410 MeV/c.

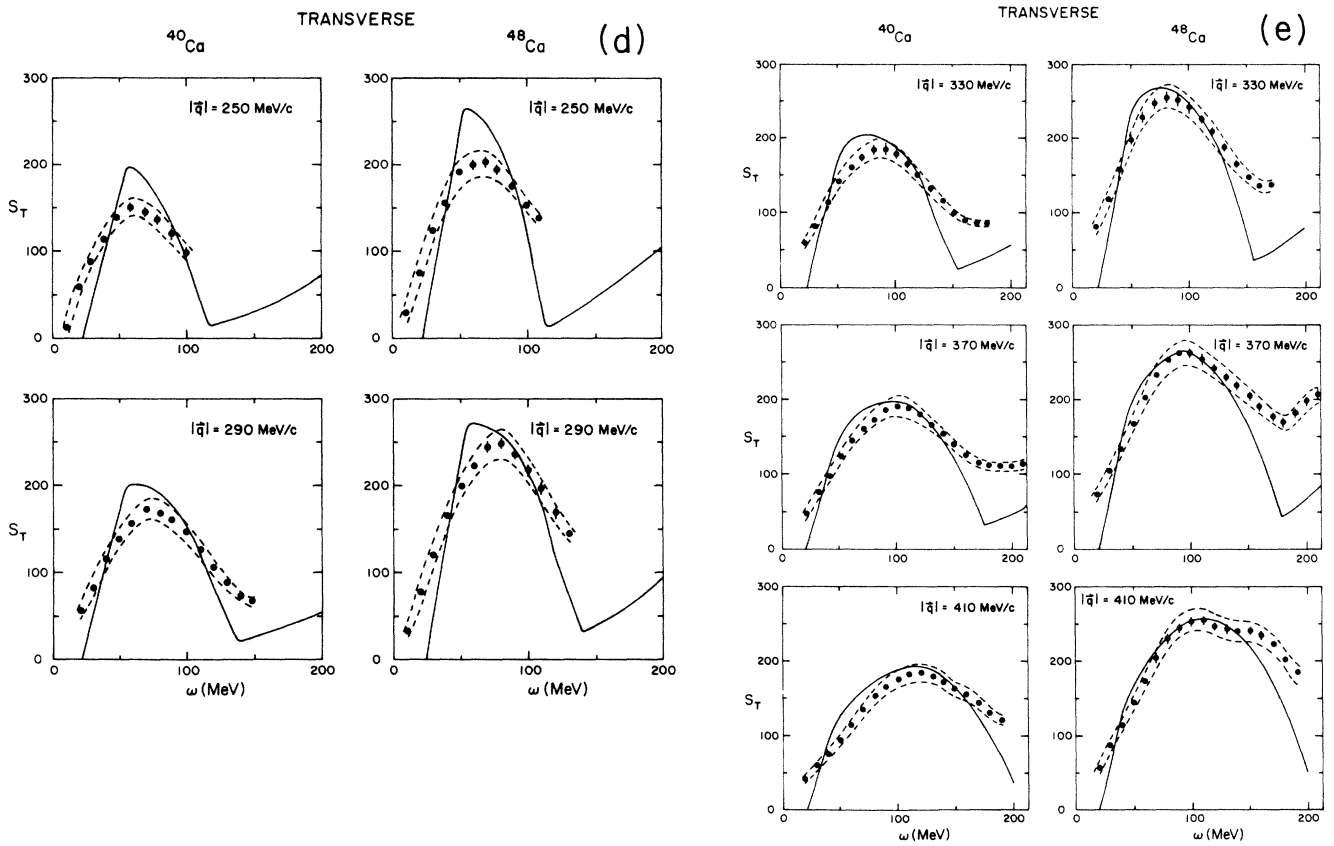

FIG. 2. (*Continued*).

Donnelly,[17] are also shown. For all of the calculations shown here, a Fermi momentum of $k=250$ MeV/c and an average nucleon binding energy of $\epsilon=23$ MeV were used. These are typical values for the calcium isotopes.[2] This fully relativistic calculation uses nucleon form factors following the parametrization of Hohler *et al.*[18] Nucleon knockout, meson exchange current, and real meson production contributions to the expected cross section are included. This is not presented as a model which should match the results in detail, but rather as a useful point of reference.

As has been seen in other recent experiments in this (q,ω) region, the transverse response function is very nearly a large, roughly parabolic peak, whose center, width, and height are given fairly well by the Fermi gas model of Van Orden. The agreement improves as q increases for both nuclei. Significant strength is seen in the large ω, "dip" region for high q, an effect which is only partially accounted for in the present calculations of mesonic effects. This effect is especially pronounced for ^{48}Ca.

As has been the case in the other experiments in which separations were performed, the longitudinal response function exhibits poorer agreement with the predictions of the Fermi gas model than does the transverse. At lower momentum transfer, the shape of the response function is decidedly unparabolic, and even the rough agreement with the shape and strength of the Fermi gas peak seen at the higher momentum transfers is not particularly good.

The longitudinal response function for ^{48}Ca is qualitatively different from that of ^{40}Ca at the higher momentum transfers. It is larger and more strongly peaked. The analysis was checked extensively for possible systematic error in the determination of the response functions of each isotope. No source of systematic error was uncovered.

As a final comparison to the Fermi gas model, an estimate of the strength of the longitudinal response function was made by integrating the measured response function over all experimentally obtainable energy losses. The results of this summation and a comparison with the sum predicted by integrating the Fermi gas response functions are given in Table I.

A recent experiment performed at Saclay has resulted in separated response functions for ^{40}Ca, ^{48}Ca, and ^{56}Fe.[8,9] Figure 3 shows a comparison of the results for $q=410$ MeV/c, where the kinematic ranges of the two experiments overlap. The agreement is generally good, although the sharply peaked structure in the Bates ^{48}Ca longitudinal response function is not seen in the Saclay results, and no apparent reason could be found for the roughly 10% difference in the ^{40}Ca transverse response functions.

ISOTOPE COMPARISON

In the kinematic region of this experiment, electron scattering is dominated by interactions with nucleons, pri-

TABLE I. Integrated longitudinal strength for ^{40}Ca and ^{48}Ca. Data were summed up to ω_{cutoff} and both statistical and systematic errors are indicated. The Fermi gas model (FGM) prediction comes from integrating the calculation of Van Orden (Ref. 17). The fraction is the ratio of data to calculation.

	q (MeV/c)	ω_{cutoff} (MeV)	Data sum$\times 10^{-4}$	FGM$\times 10^{-4}$	Fraction
^{40}Ca	250	100	2.20±0.02±0.31	3.00	0.73±0.01±0.11
	290	150	2.29±0.03±0.43	3.01	0.76±0.01±0.14
	330	180	1.74±0.03±0.49	2.92	0.60±0.01±0.17
	370	230	1.54±0.05±0.64	2.75	0.56±0.02±0.23
	410	190	1.48±0.04±0.51	2.51	0.59±0.02±0.20
^{48}Ca	250	110	3.18±0.05±0.47	3.60	0.88±0.01±0.13
	290	130	2.50±0.05±0.54	3.62	0.69±0.01±0.15
	330	170	2.70±0.06±0.69	3.51	0.77±0.02±0.19
	370	190	2.42±0.07±0.39	3.30	0.73±0.02±0.22
	410	190	2.16±0.06±0.75	3.02	0.72±0.02±0.26

marily single nucleon knockout. The 40% increase in the neutron number of ^{48}Ca relative to ^{40}Ca provides a unique opportunity to observe any effect that is strongly dependent on the neutron number. A comparison of the Fermi gas calculations, for example, shows that the theoretical response functions in the two isotopes are very similar, ^{40}Ca being essentially a scaled down version of ^{48}Ca. The

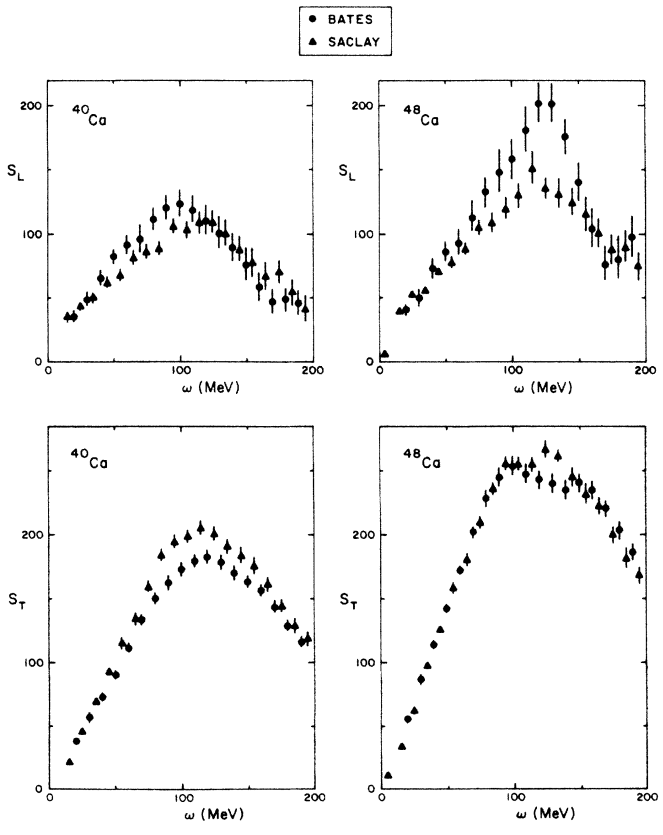

FIG. 3. Separated response functions for $q=410$ MeV/c. The circles indicate the results of this paper, the triangles are points taken from the results of Mezziani *et al.* (Refs. 8 and 9). Statistical error bars only are shown.

scale factor is found to be 0.83 for the longitudinal response and 0.74 for the transverse. Other effects, such as mesonic degrees of freedom, would be expected to exhibit a more complicated signature.

As a way of comparing the two isotopes, the ^{48}Ca response functions were "renormalized" by the ratio of the maximum values of the Fermi gas calculations for each isotope. The results of plotting the renormalized ^{48}Ca response functions versus the ^{40}Ca response functions is shown in Fig. 4 for representative "low" and "high" values of q.

Both longitudinal and transverse response functions roughly scale at low momentum transfers. At higher q, the ^{48}Ca exhibits a greater strength in the large ω region, possibly due to nucleonic excitations, which would not be expected to scale as nucleon knockout response functions. The high q longitudinal response functions exhibit the greatest isotopic discrepancy, with the peaking structure which develops in ^{48}Ca largely absent in the response functions of ^{40}Ca.

A second difference in the isotopes is seen at the highest momentum transfers covered in this experiment. These data, shown in Fig. 5 plotted against Fermi gas calculations of the total cross section, come from spectra taken at a scattering angle of 140° and $E_0=330$ and 370 MeV, the highest initial electron energies at 140° scattering angle. Since no corresponding points at 90° were obtainable with the electron energies then available at Bates, these points are not included in the separations, but at 140° the response is primarily transverse. The center of the peaks are at $q=500$ and 550 MeV/c, respectively.

At the high momentum transfer, the Fermi gas model underestimates the ^{48}Ca data severely, accounting for less than 70% of the observed cross section at the center of the peak. This response in excess of that predicted by the Fermi gas is less evident at the lower momentum transfer in ^{48}Ca and is just noticeable at the highest momentum transfer in ^{40}Ca. The only data taken in this experiment at still higher momentum transfers are spectra taken at 160° for which not all corrections could be performed. These seem to corroborate the interpretation that this enhancement of the cross section increases as q increases

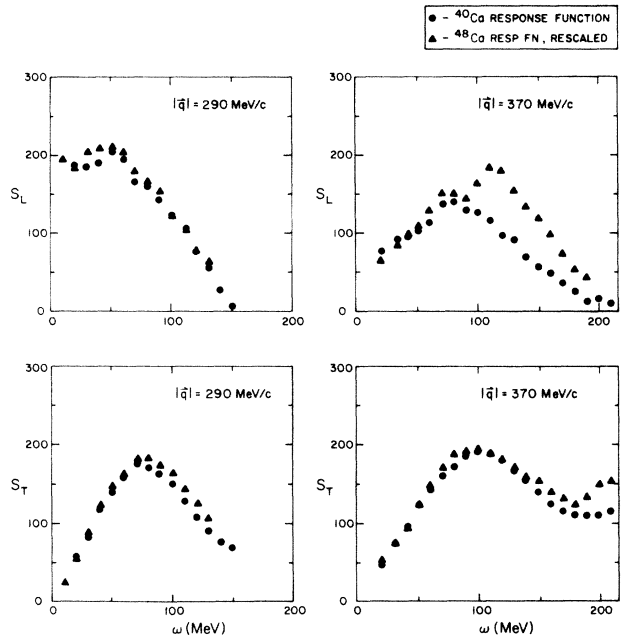

FIG. 4. Separated response functions, with those of ^{48}Ca scaled by the ratio of the Fermi gas calculations (0.83 for longitudinal, 0.74 for transverse).

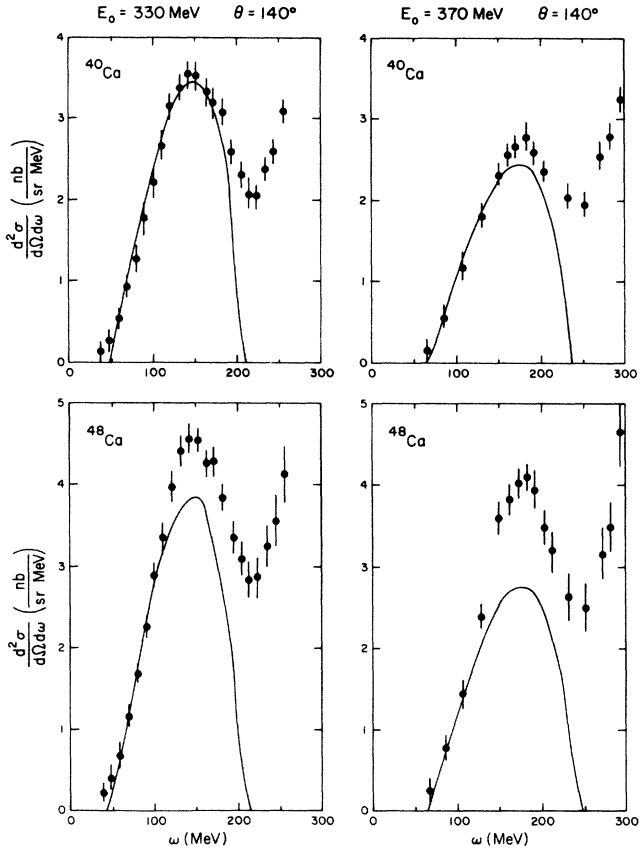

FIG. 5. Fully corrected cross sections for $\theta = 140°$, $E_0 = 330$ and 370 MeV, compared with the Fermi gas calculation for nucleon knockout by Van Orden.

and is larger in ^{48}Ca than it is in ^{40}Ca for the same kinematics.

It would seem worthwhile to search for an explanation of this isotopic difference in terms of mesonic effects. The calculations of Van Orden shown at lower values of q in Fig. 2 would indicate that this may not be the case. While meson production is more prevalent in ^{48}Ca than in ^{40}Ca, these calculations do not show as dramatic a difference as is seen in these 140° data. In particular, nothing immediately accounts for the fact that the excess strength is evident at a lower value of q in ^{48}Ca than it is in ^{40}Ca.

CONCLUSIONS

The results can be summarized as follows. For momentum transfers in the range 250—400 MeV/c, and energy losses less than 200 MeV, both ^{40}Ca and ^{48}Ca have transverse deep inelastic response functions which behave much as one would expect from a single nucleon knockout picture such as that the Fermi gas model provides. Such a model is not sufficient to explain the increase in the cross section at higher q and ω, effects possibly due to mesonic or nucleonic degrees of freedom. For the longitudinal response function, neither isotope has a response function that matches the nucleon knockout model, although each exhibits a peaked structure at higher momentum transfers. In both longitudinal and transverse responses, those characteristics which seem to predominate at higher q are more pronounced in ^{48}Ca than in ^{40}Ca.

An initial comparison of the response functions for two particular isotopes at energies that do not allow a full sampling of the delta region is bound to raise more questions than it answers. Fortunately, experiments are being planned that will sample a larger range of q and ω. From these, it should be possible to determine whether the effects seen here are precursors of more general properties of deep inelastic response functions or not. The A dependence of the response functions in this region should give some insight into the origins of those effects that are not easily explained by single nucleon knockout.

Experience in deep inelastic scattering experiments leads one to an inescapable conclusion: they are difficult to perform. The number of corrections performed on the data result in larger error bars than one would like. On the positive side, future experimenters will be able to anticipate the possible background sources better and the results should be more reliable. This is especially true for a good determination of the longitudinal response function, which will depend on the availability of higher energy data at more forward angles.

ACKNOWLEDGMENTS

The authors would like to thank J. W. Van Orden for the theoretical calculations used in this paper and T. W. Donnelly for many fruitful discussions about theoretical

implications. They are indebted to J. LeRose for assistance in the data analysis and interpretation. The staff at the Bates Linear Accelerator Center provided excellent experimental support. Special thanks goes to J. Morgenstern for providing tables of the Saclay results for a comparison. The Louisiana State University group was supported in part by the National Science Foundation. The Massachusetts Institute of Technology and University of Virginia groups were supported in part by the United States Department of Energy under Contracts EY-76-C-02-3069 and DE-AS05-78ER05861, respectively.

---

*Present address: Department of Physics, Mount Holyoke College, South Hadley, MA 01075.

[1]R. R. Whitney *et al.*, Phys. Rev. C **9**, 2230 (1974).
[2]P. D. Zimmerman and M. R. Yearian, Z. Phys. A **278**, 291 (1976).
[3]E. Moniz *et al.*, Phys. Rev. Lett. **26**, 445 (1971).
[4]T. W. Donnelly, Nucl. Phys. **A150**, 393 (1970).
[5]T. deForest, Nucl. Phys. **A132**, 305 (1969).
[6]P. Barreau *et al.*, Nucl. Phys. **A402**, 515 (1983).
[7]M. Deady *et al.*, Phys. Rev. C **28**, 631 (1983).
[8]Z. E. Mezziani *et al.*, Phys. Rev. Lett. **52**, 2130 (1984).
[9]Z. E. Mezziani *et al.*, Phys. Rev. Lett. **54**, 1233 (1985).
[10]C. Blatchley, Ph.D. thesis, Lousiana State University, 1985 (unpublished).
[11]W. Bertozzi *et al.*, Nucl. Instrum. Methods **141**, 457 (1977).
[12]C. F. Williamson, Bates Linear Accelerator Center Internal Report 82-06, 1982.
[13]L. W. Mo and Y. S. Tsai, Rev. Mod. Phys. **41**, 205 (1969).
[14]J. LeRose *et al.*, Phys. Rev. C **32**, 449 (1985).
[15]G. Miller, Stanford Linear Accelerator Center Report SLAC-PUB-848, 1971.
[16]Y. Kawazoe, G. Takeda, and H. Matsuzaki, Prog. Theor. Phys. **54**, 1394 (1975).
[17]J. W. Van Orden and T. W. Donnelly, Ann. Phys. (N.Y.) **131**, 451 (1980).
[18]G. Hohler *et al.*, Nucl. Phys. **B114**, 505 (1976).